

Magnetic behavior of the heavy-fermion system UPd₂Ga₃

S. Süllow, B. Ludoph, B. Becker, G. J. Nieuwenhuys, A. A. Menovsky, and J. A. Mydosh
Kamerlingh Onnes Laboratory, Leiden University, 2300 RA Leiden, The Netherlands

S. A. M. Mentink and T. E. Mason
Department of Physics, University of Toronto, Toronto, Canada M5S 1A7
 (Received 17 May 1995)

We have synthesized the heavy-fermion compound UPd₂Ga₃, crystallizing in a structure closely related to the hexagonal PrNi₂Al₃ lattice. The physical properties show UPd₂Ga₃ to behave very similar to the heavy-fermion superconductor UPd₂Al₃. It orders antiferromagnetically at $T_N=13$ K, while a large decrease in the electrical resistivity below T_N and electronic specific-heat coefficient $\gamma=230$ mJ/mol K² classify the new compound as a heavy fermion. The magnetic structure is equivalent to that of UPd₂Al₃, although the ordered moment of $0.50(5)\mu_B$ is smaller. No superconductivity has been observed in UPd₂Ga₃ above 50 mK.

I. INTRODUCTION

Heavy-fermion materials are of general interest in present day research due to their unusual and still not fully understood low-temperature properties. Many of these systems order magnetically, and some become superconducting as well. Two of the more recent examples are UPd₂Al₃ and UNi₂Al₃. Both systems crystallize in the hexagonal PrNi₂Al₃ structure, show magnetic transitions at 14.5 and 4.6 K, and become superconducting below 2 and 1 K, respectively.^{1,2} It has been argued that in UPd₂Al₃ superconductivity and magnetism are carried by different electronic f subsystems of "light" magnetic ($\gamma=25$ mJ/mol K²) and "heavy" superconducting character ($\gamma=115$ mJ/mol K²).^{3,4}

In this contribution we present our results on the allomorphic compound UPd₂Ga₃. We were able to prepare this material in nearly single-phase polycrystalline form and determine its crystal structure. Our measurements of the specific heat, electrical resistivity, magnetoresistivity, magnetic susceptibility, magnetization, and neutron diffraction show UPd₂Ga₃ to order antiferromagnetically at $T_N\approx 13$ K. No superconductivity was observed down to 50 mK. The zero-temperature extrapolation of the specific heat c_p/T is 230 mJ/mol K², thus making UPd₂Ga₃ a moderately heavy-fermion material. The resistivity exhibits a large drop below T_N , which indicates that a very large scattering contribution is removed by a continuous formation of a coherent state and the magnetic ordering.

These and the other physical properties of UPd₂Ga₃ will be compared to those of UPd₂Al₃ in which superconductivity does coexist with magnetism. We will discuss both systems and give arguments for the similarities of the magnetic and disparity of the superconducting properties in terms of the differences of the crystal structures affecting the Fermi surface.

II. METALLURGY AND EXPERIMENTAL TECHNIQUES

Polycrystalline samples of UPd₂Ga₃ have been formed by arc-melting the constituents (with purity U: 3N, Pd: 5N, and

Ga: 4N) in stoichiometric ratio under argon atmosphere in a water-cooled copper crucible. The weight loss during melting was less than 0.5%. Subsequently the samples were annealed for one week at 700 °C in high vacuum in a quartz ampule. As-cast and annealed material has been examined by electron-probe microanalysis. This proved that annealing is necessary to obtain a homogeneous sample of the proper stoichiometry. While as-cast samples consist of about 70 vol. % of a phase with the composition UPd_{2.4}Ga_{3.2} and 30 vol. % UPd_{1.2}Ga_{2.4}, the annealed samples contain 95% UPd₂Ga₃, 4 vol. % UPd_{2.6}Ga_{3.4}, and 1 vol. % UGa₃.

The crystallographic structure has been determined by a full refinement of combined x-ray and neutron diffraction at room temperature, and refinement of further neutron diffractograms at 4.2, 20, and 150 K. Best agreement between calculated and measured diffraction patterns was achieved by assuming a hexagonal superstructure of the PrNi₂Al₃ lattice with the unit cell doubled along the c axis (BaB₂Pt₃ structure). The lattice parameters at room temperature are $a=5.3015(1)$ Å and $c=8.5112(3)$ Å. Details of the structure, including the free positional parameters of Pd and Ga are given in Table I. The superstructure is realized by the small displacement of the Ga and Pd atoms. In the

TABLE I. Refined structural parameters of UPd₂Ga₃, space group $P6_3/mmc$ (BaB₂Pt₃ type), from neutron powder diffraction at $T=290, 150,$ and 20 K. The room-temperature refinement is the result of a refinement of combined neutron and x-ray powder diffraction patterns.

	$T=290$ K	$T=150$ K	$T=20$ K
a (Å)	5.3015(1)	5.2904(3)	5.2840(3)
c (Å)	8.5112(3)	8.4834(8)	8.4774(9)
V (Å ³)	207.17(2)	205.63(2)	204.98(2)
x_{Ga} (-)	0.5055(4)	0.5118(7)	0.5106(7)
y_{Ga} (-)	0.0110(8)	0.024(1)	0.021(1)
z_{Pd} (-)	0.0262(2)	0.0185(7)	0.0197(7)
R_p (%)	16.3	17.3	18.6
Ordered moment at 4.2 K: $0.50(5)\mu_B/\text{U atom}$			

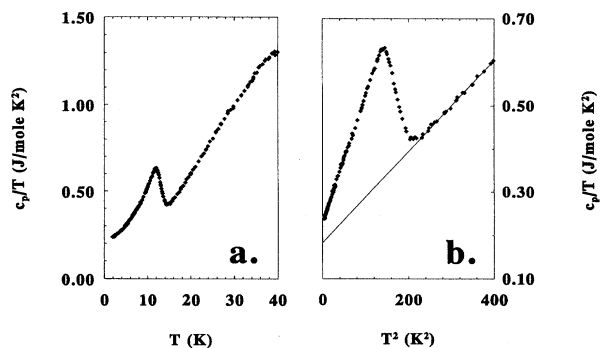


FIG. 1. (a) The specific heat c_p/T vs T of UPd₂Ga₃. (b) The specific heat c_p/T vs T^2 . The solid line indicates the influence of CEF contributions on the determination of γ ; the extrapolation between 15 and 20 K leads to a lower value of γ than the extrapolation between 1.8 and 10 K.

PrNi₂Al₃ lattice the positions of the Ga and Pd atoms would be given by parameter values x_{Ga} , y_{Ga} , and z_{Pd} of 0.5, 0, and 0, respectively. We have not been able to determine the crystallographic structure of the UPd_{2.6}Ga_{3.4} impurity phase. Since we have not excluded the reflections corresponding to this phase, the reliability factors of our refinement are rather poor.

There are obvious differences in the lattice constants between UPd₂Ga₃ and UPd₂Al₃; for UPd₂Al₃ values of 5.365 Å (a axis) and 4.186 Å (c axis) have been reported.¹ Thus, while half the c axis of UPd₂Ga₃ is nearly 2% longer than that of UPd₂Al₃, the a axis is about 1% shorter. On the one hand, this implies a larger magnetic anisotropy between hexagonal plane and c axis in UPd₂Ga₃ compared to UPd₂Al₃, on the other hand it gives rise to a stronger U-Pd hybridization, since the distance between U and Pd is considerably diminished here (UPd₂Ga₃: 3.069 Å vs UPd₂Al₃: 3.097 Å).

Moreover, the unit-cell volume of the Ga compound is reduced compared to the Al system. While for UPd₂Ga₃ half the volume of the unit cell is $V=103.6 \text{ \AA}^3$, it is $V=104.3 \text{ \AA}^3$ for UPd₂Al₃. Generally, such change of the unit-cell volume can be treated in terms of increasing the hybridization on applying pressure. Although the volume effect is generated by anisotropic lattice parameter changes (i.e., by uniaxial pressure), we can at least estimate the order of magnitude of (hydrostatic) pressure necessary to achieve a similar compression. With the isothermal compressibility $\kappa_T=0.85 \text{ Mbar}^{-1}$ of UPd₂Al₃ this volume difference between the two systems would be equivalent to 10 kbar pressure applied to UPd₂Al₃.⁵

The physical properties of UPd₂Ga₃ have been examined by specific heat c_p , resistivity ρ , susceptibility χ , magnetization M , and neutron diffraction. The specific heat has been determined by a conventional adiabatic technique, at temperatures from 1.8 to 50 K. The resistivity was measured with a four-probe ac technique in zero field from 50 mK to 300 K and in fields up to 8.5 T below 1.5 and 16 K utilizing a four-probe dc technique. For the susceptibility in 0.01 T between 2 and 300 K, a commercial SQUID was employed,

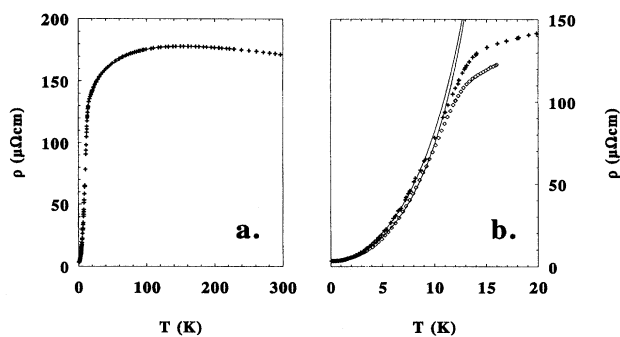


FIG. 2. (a) The overall behavior of the resistivity of UPd₂Ga₃. (b) The low-temperature resistivity ρ of UPd₂Ga₃ in zero field (+) and in a field of 8 T (\diamond) with the magnetic transition. In the zero-field measurement the resistivity drops by a factor of 40 between 14 and 0.05 K. The solid lines are fits to Eq. (1) with parameters as described in the text.

while the magnetization was obtained using a FONER magnetometer between 5 and 15 K from 0 to 12 T. Powder neutron-diffraction measurements were performed with the high-resolution 800-wire multidetector on the C2 spectrometer at the NRU reactor of Chalk River Laboratories, using a neutron wave length of 1.5405 Å. The 1-cm³ sample was mounted in a cylindrical vanadium container with helium exchange gas. Full diffractograms were recorded at temperatures from 4 to 290 K.

III. RESULTS

The specific heat divided by temperature in zero field vs temperature T is plotted in Fig. 1(a). An anomaly (of antiferromagnetic origin, as will be shown below) is clearly visible, the transition temperature is determined by an entropy balance to $T_N=13.3$ K. At higher temperatures the c_p/T vs T curve starts to bend due to contributions of crystalline electric fields (CEF). The CEF contributions prohibit an evaluation of the electronic specific heat γ at temperatures above T_N . Extrapolating c_p/T between 15 and 20 K to $T=0$, as is done by the straight line in Fig. 1(b) (where c_p/T is plotted against T^2), leads to a γ that is lower than that yielded by an extrapolation from below 10 K, thus illustrating the influence of CEF contributions above T_N on the determination of γ . From the low-temperature extrapolation we obtain $\gamma=230 \text{ mJ/mol K}^2$ indicating that UPd₂Ga₃ belongs to the class of heavy-fermion materials [for comparison the value of UPd₂Al₃: $\gamma=140 \text{ mJ/mol K}^2$ (Ref. 3)]. We did not correct the specific heat of UPd₂Ga₃ for lattice contributions, since up to now no nonmagnetic allomorph having a superstructure as described above has been found and thus we cannot obtain a reliable correction for the phonons. We remark that, although there are quantitative differences between the specific heat of UPd₂Ga₃ and UPd₂Al₃, the general shape of c_p is quite similar for both systems.

The resistivity in zero field of UPd₂Ga₃ closely resembles that of UPd₂Al₃ [Fig. 2(a)]. The broad maximum around 150 K with the downturn at lower temperatures is

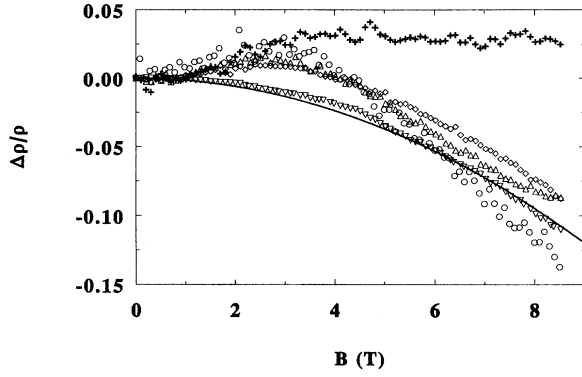


FIG. 3. The normalized magnetoresistivity of UPd₂Ga₃ at 15 K (∇), 12 K (◇), 8 K (△), 5 K (○), and 1.6 K (+). The solid line indicates a B^2 dependence of the magnetoresistivity of the measurement at 15 K.

assigned to the Kondo effect with its reduction due to the low-temperature coherent state and to the depopulation of CEF levels. However, before the coherent state can fully form, magnetic ordering appears. T_N for $B=0$ T is determined to be 13.1 K, defined as the minimum in $d^2\rho/dT^2$, which corresponds to the kink in ρ [Fig. 2(b)]. With magnetic field only a slight decrease of T_N is observed, at 8 T we find a value of 12.3 K.

As in the case of UPd₂Al₃, the zero field resistivity ρ_{ZF} shows a dramatic decrease from just above T_N to lowest temperatures. For UPd₂Ga₃ the resistivity drops by a factor of 40 between 14 and 0.05 K. Dissimilar to UPd₂Al₃, no sign of superconductivity is observed in UPd₂Ga₃ down to lowest attainable temperature (50 mK). Following the approach of Caspary *et al.*³ we fit ρ_{ZF} below 10 K with a power law

$$\rho(T) = \rho_0 + AT^2 + bT^5 \quad (1)$$

with $\rho_0 = 3.37(3) \mu\Omega \text{ cm}$, $A = 0.663(5) \mu\Omega \text{ cm K}^{-2}$, and $b = 0.12(1) \times 10^{-3} \mu\Omega \text{ cm K}^{-5}$. Caspary *et al.*³ derived fit parameters of $\rho_0 = 9.2 \mu\Omega \text{ cm}$, $A = 0.26 \mu\Omega \text{ cm K}^{-2}$, and $b = 0.48 \times 10^{-3} \mu\Omega \text{ cm K}^{-5}$, qualitatively illustrating the similarities below T_N of UPd₂Ga₃ and UPd₂Al₃. With our data we can calculate the ratio A/γ^2 yielding a value of $12.5 \mu\Omega \text{ cm (mol K/J)}^2$. This number is in good agreement with that of other heavy-fermion systems [CeAl₃: $A/\gamma^2 = 13.3 \mu\Omega \text{ cm (mol K/J)}$ (Ref. 6)], proving that A is really reflecting the heavy mass of the electrons. We also note that the number A we derived for UPd₂Ga₃ is 2.5 times larger than that one given for UPd₂Al₃, this in good agreement with the difference between the two γ values.

The same fit procedure can be performed for the resistivity measured in a magnetic field of 8 T. A best fit of the resistivity below 10 K was obtained using parameters of $\rho_0 = 3.37(3) \mu\Omega \text{ cm}$, $A = 0.556(6) \mu\Omega \text{ cm K}^{-2}$, and $b = 0.15(1) \times 10^{-3} \mu\Omega \text{ cm K}^{-5}$. From the fit parameters it is obvious that the magnetic field has mainly influenced the T^2 term.

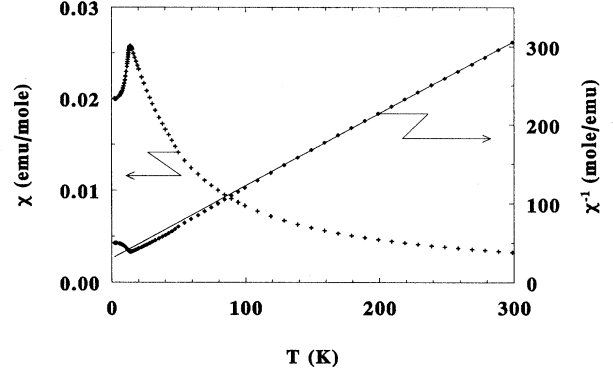


FIG. 4. The susceptibility χ and the inverse susceptibility χ^{-1} of UPd₂Ga₃ plotted against temperature. The solid line indicates a Curie-Weiss fit of the data with $\mu_{\text{eff}} = 2.95\mu_B$ and $\Theta_{\text{CW}} = -33$ K.

To examine this influence in more detail we performed measurements of the magnetoresistivity in fields up to 8.5 T. In Fig. 3, we show the normalized magnetoresistivity $\Delta\rho/\rho_{ZF} = [\rho(B) - \rho_{ZF}]/\rho_{ZF}$ at different temperatures. Two effects can be distinguished: (i) Above T_N the resistivity decreases with B^2 (the solid line in Fig. 3 indicates a B^2 dependence of the magnetoresistivity at 15 K). (ii) At 1.6 K the resistivity shows, instead of a decrease, a small increase with field. In the intermediate temperature range both effects contribute to the magnetoresistivity leading to a maximum in $\Delta\rho/\rho_{ZF}$.

The negative $\Delta\rho/\rho_{ZF}$ at high temperatures can have two sources, either spin disorder scattering is removed by the field or the field is affecting the coherent state. Both effects should be $\propto B^2$, and therefore, we cannot separate the two. On the other hand, the small magnetoresistivity at 1.6 K is entirely due to the field trying to rearrange the antiferromagnetic moments. Hence, the low-temperature magnetoresistivity reveals a complicated interplay between the influence of magnetic field on the coherent state, on the one hand, and on the magnetic moments on the other. We note that the magnetoresistivity of UPd₂Ga₃ resembles qualitatively that one of UPd₂Al₃ determined by de Visser *et al.*⁷ for a single crystal with the current and the field oriented along the a axis (i.e., the low resistive axis). The small influence of a magnetic field of 8 T on T_N of UPd₂Ga₃ suggests a phase diagram similar to that of UPd₂Al₃. Taken together the experiments on resistivity and magnetoresistivity indicate that there is a continuous development of the coherent state below T_N and that the very large drop in the electrical resistivity upon antiferromagnetic order is not solely due to the decrease of spin-disorder scattering.

In order to clarify the nature of the magnetic transition we measured the susceptibility χ . In Fig. 4, we plot our data both as χ and χ^{-1} vs T . At high temperatures the susceptibility follows a Curie-Weiss law with an effective moment $\mu_{\text{eff}} = 2.95\mu_B$ and $\Theta_{\text{CW}} = -33$ K (by extrapolating χ^{-1} above 100 K as straight line). This effective moment is in agreement with the expected value for either a free U³⁺ or U⁴⁺ atom. The negative Curie-Weiss temperature, indicative of antiferromagnetic coupling, is in accord with the antifer-

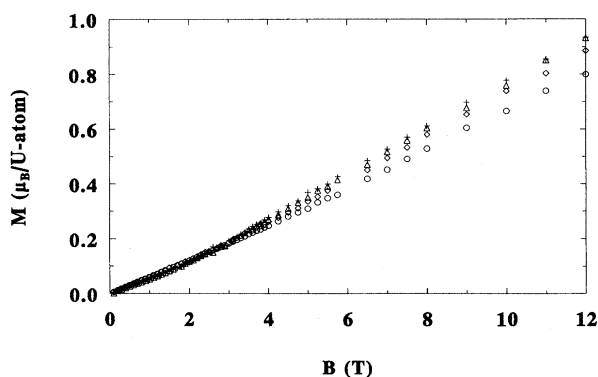


FIG. 5. The magnetization of UPd₂Ga₃ in fields up to 12 T. The measurements have been taken at 15 K (○), 12 K (◇), 8 K (△), and 5 K (+).

romagnetic peak at $T_N=12.2$ K [determined as maximum in $d(\chi T)/dT$]. The transition temperature derived from the susceptibility is somewhat lower than those extracted from specific heat or resistivity: This is probably due to the relatively broad transition [see the specific heat (Fig. 1)] blurring the exact determination of the transition temperature in the various measurements.

Unlike UPd₂Al₃ there is no pronounced maximum in the susceptibility for UPd₂Ga₃ above T_N , which for the Al compound was attributed to CEF contributions. In UPd₂Ga₃ this maximum is hidden behind the antiferromagnetic transition and is visible here only as small anomaly in χ^{-1} . Qualitatively the susceptibility of UPd₂Ga₃ can be explained within a CEF scheme as proposed by Grauel *et al.*⁸ for UPd₂Al₃ but now with a singlet ground state, an excited singlet at about 15 K and a further doublet around 60 K. Especially, we note that the susceptibility for $T \rightarrow 0$, χ_0 , being about two times larger for the Ga system than for the Al compound, arises from those low-lying CEF levels. However, without data on the anisotropy of the physical properties, we are unable to obtain more quantitative information about the crystalline electric fields in UPd₂Ga₃.

Further, we measured the magnetization of UPd₂Ga₃ between 5 and 15 K in fields up to 12 T (Fig. 5). The magnetization at 12 T is about $0.8\text{--}0.9\mu_B/\text{U}$ atom and shows no sign of saturation. The absolute values of M for UPd₂Ga₃ are larger than those of UPd₂Al₃ [$\approx 0.3\mu_B$ at 10 T, determined for a single crystal with a $B\parallel a$ axis (Ref. 9)]. This is a consequence of the smaller CEF splitting in UPd₂Ga₃ compared to UPd₂Al₃. M seems initially linear in B for all temperatures. However, a slight upward curvature begins at lower and lower field as the temperature is reduced. This behavior might arise from domain reorientation processes, as they have been found for UPd₂Al₃ in the same temperature and field range.⁸

In order to determine the magnetic structure of UPd₂Ga₃, we performed a neutron-diffraction study.¹⁰ Full diffractograms were recorded from $2\theta=5^\circ\text{--}85^\circ$ at temperatures from 4.2–20 K. In the difference spectrum of $I(4.2\text{ K})-I(20\text{ K})$ four extra reflections are observed, which are indexed as the (001), (101), (111), and (103) reflections of a

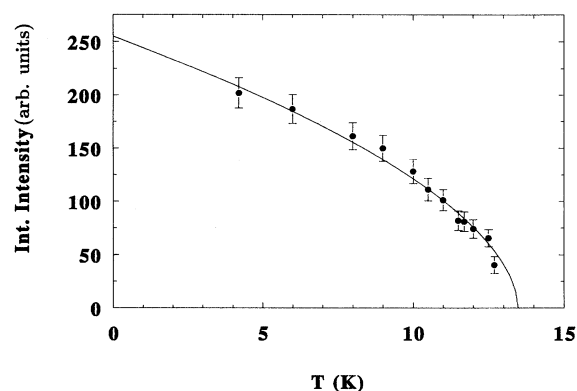


FIG. 6. Integrated intensity vs temperature of the magnetic (001) reflection of UPd₂Ga₃. The solid line denotes a fit to Eq. (2), yielding $\beta=0.28(2)$.

magnetic unit cell equal to the nuclear unit cell, $a_{\text{magn}}=a_{\text{nucl}}=5.286$ Å and $c_{\text{magn}}=c_{\text{nucl}}=8.474$ Å. The ordering wave vector is (001), implying that ferromagnetic planes are stacked antiferromagnetically along the c axis. The integrated intensities of these magnetic reflections closely agree with those calculated for an ordered structure in which uranium moments are restricted to the basal plane. The orientation of the moment in the basal plane cannot be determined from our powder experiment. This magnetic structure is the same as that of UPd₂Al₃.¹¹ The ordered moment at 4.2 K is evaluated from a comparison of the integrated intensities of the (001) and (101) magnetic reflections with the nuclear (200) and (202) reflections, using the reported uranium form factor.¹² This procedure yields $\mu_{\text{ord}}(4.2\text{ K})=0.50(5)\mu_B/\text{U}$ atom, well above the detection limit of our powder-diffraction experiment, which is about $0.15\mu_B$. The small U moment explains the absence in the difference spectrum of the other reflections of this magnetic structure. Figure 6 displays the temperature evolution of the integrated intensity of the (001) magnetic reflection. The temperature dependence can be nicely described by the expression

$$I=A\left(\frac{T_N-T}{T_N}\right)^{2\beta}, \quad (2)$$

where β is the critical exponent for the ordering and A a scaling factor. We find $T_N=13.4(2)$ K and $\beta=0.28(2)$. This value is suggestive of conventional 3D XY ordering for UPd₂Ga₃.

The ordered moment μ_{ord} being considerably smaller than the moment of UPd₂Al₃ ($0.85\mu_B$) is in agreement with the observation of the higher effective masses in UPd₂Ga₃ (higher density of states at the Fermi level), since stronger screening is to be expected. Also, a smaller ordered moment is expected from the differences of the crystal structures between the two systems, because, as remarked, in UPd₂Ga₃ the U-Pd distance is smaller than in the Al allomorph leading to a stronger hybridization of the moments. However, one would expect that with a substantially smaller moment also the transition temperature T_N should be correspondingly re-

duced. This, obviously, is not the case. We remark that this rule of the dependence of T_N on the ordered magnetic moment is broken for several heavy-fermion compounds. For instance, URu₂Si₂ has an even higher T_N than UPd₂Al₃, but the ordered magnetic moment is only $0.03\mu_B$.¹³

IV. CONCLUSIONS

We have presented a study of the metallurgical and physical properties of the new heavy-fermion compound UPd₂Ga₃. This compound crystallizes in the BaB₂Pt₃ structure, a superstructure of the PrNi₂Al₃ type. With respect to the heavy-fermion superconductor UPd₂Al₃ the major differences are that (a) the volume of the unit cell is decreased, (b) the lattice constants change anisotropically, and (c) the superstructure causes a doubling of the unit cell along the *c* axis and slight modifications of the local site symmetry of the U atom.

The bulk properties show that UPd₂Ga₃ is a heavy-fermion system with an antiferromagnetic phase transition at $T_N \approx 13$ K, while it is not superconducting above 50 mK. The appearance of the magnetic transition in the bulk properties of UPd₂Ga₃ resembles qualitatively that in UPd₂Al₃. The quantitative differences can be accounted for by the larger effective mass of the electrons and a smaller CEF splitting in case of UPd₂Ga₃. Further, the magnetic structures of UPd₂Ga₃ and UPd₂Al₃ are identical.

(a) The decrease of the unit-cell volume of UPd₂Ga₃. To a first approximation this can be viewed as hydrostatic pressure applied to UPd₂Al₃. The decrease of the unit-cell volume of nearly 1% corresponds to a pressure of about 10 kbar. Pressure experiments on UPd₂Al₃ revealed only negligible pressure dependences of the transition temperatures T_N and T_c in this pressure regime.^{3,5} Therefore, something more is needed to explain the loss of superconductivity in UPd₂Ga₃ than simple chemical pressure as, for example, Fermi-surface effects. Here, band-structure calculations of UPd₂Ga₃ would give valuable information especially if compared to those for UPd₂Al₃.¹⁴

(b) The anisotropic change of lattice parameters or the increasing U-Pd hybridization. This feature can nicely account for the differences of the magnetic behavior of the two systems. A stronger U-Pd hybridization explains the larger γ and the smaller ordered magnetic moment μ_{ord} . The comparatively small decrease of T_N (with respect to the larger decrease of μ_{ord}) can qualitatively be interpreted within the model put forth by Mentink *et al.*¹⁵ for CePd₂Al₃. These authors proposed that in the hexagonal 123-compounds magnetism is governed by an interplay of the in-plane ferromagnetic coupling and the interplane antiferromagnetic interaction. Within their model the antiferromagnetic transition temperature T_N is then determined by the interplane exchange parameter J_z and the spin value of the basal plane magnetic moment, $S(S+1)$. Comparing now the Al system with the Ga homologue, the spin value S of UPd₂Ga₃ is lowered, while J_z is increased due to the larger Ga atom creating a larger $f-s,p$ overlap. Accordingly, T_N depends on two competing effects, and, in our case, is only slightly lowered. We remark that a similar dependence of J_z on the $f-s,p$ overlap has been observed in CePd₂Al₃ and CePd₂Ga₃.^{15,16}

However, although the magnetic behavior of UPd₂Ga₃ can be fairly well explained within such models, the complete absence of superconductivity is far from evident within these models. At present we can only speculate about a possible connection between the anisotropy-hybridization changes in UPd₂Ga₃ and the $2-f$ subsystem model.^{3,4} It is striking that in UPd₂Ga₃ as in UPd₂Al₃ the magnetic behavior seems essentially independent of the absence or presence of superconductivity. For now, at best, we can only propose an experimental test for the role of the U-Pd hybridization. The test would be an uniaxial pressure experiment on UPd₂Al₃ with the pressure applied along the *c* axis.

In our model, described above, T_N is dependent on J_z and S . Uniaxial pressure along the *c* axis should increase both J_z (since the $f-s,p$ overlap gets stronger) and S (since the U-Pd hybridization becomes weaker). Hence, T_N would increase with uniaxial pressure along the *c* axis for UPd₂Al₃. The role of the hybridization change on the superconductivity should also be reflected in the uniaxial pressure dependence of T_c . If the U-Pd distance is critical for the suppression of superconductivity in UPd₂Ga₃, then T_c of UPd₂Al₃ should be independent of or even increase with uniaxial pressure applied to the *c* axis.

(c) The crystallographic superstructure and the increase of atomic weight by the substitution of Ga for Al. The crystallographic superstructure might affect the physical properties of UPd₂Ga₃ by two different ways. First, it will slightly change the local site symmetry of the U atoms, and accordingly modify the Fermi surface. Unfortunately, from our data we cannot assess the importance of the local site symmetry for the physical properties of UPd₂Ga₃. Second, the phonon spectrum might possibly be changed by the superstructure, and there will surely be an influence on the phonons by the substitution of Ga for Al, since Ga is about 2.5 times heavier than Al. This, of course, implies a simple BCS picture for superconductivity in UPd₂Al₃ and superconductivity in UPd₂Ga₃ would be destroyed by modifying the phonon spectrum.

In conclusion, based upon our experimental data, we believe a picture using the U-Pd hybridization and the interplane exchange mediated by the Ga or Al atoms can give a reasonable description of the magnetic behavior in these two materials. However, as far as the superconductivity is concerned we have been unable to determine the key parameter for its suppression in UPd₂Ga₃. It is quite possible that all effects mentioned above play a collective role. At any rate, we propose a uniaxial pressure experiment in UPd₂Al₃ which would shed more light on the anisotropy-hybridization situation. Finally the band structure of UPd₂Ga₃ should be calculated and compared with UPd₂Al₃.

ACKNOWLEDGMENTS

We would like to thank R. Donaberger for assistance with the neutron-scattering measurements. This work was partially supported by the Nederlandse Stichting voor Fundamenteel Onderzoek der Materie (FOM), the Canadian Institute for Advanced Research and the Natural Sciences and Engineering Research Council. The samples were prepared in FOM-ALMOS.

- ¹C. Geibel, C. Schank, S. Thies, H. Kitazawa, C. D. Bredl, A. Böhm, M. Rau, A. Grauel, R. Caspary, R. Helfrich, U. Ahlheim, G. Weber, and F. Steglich, *Z. Phys. B* **84**, 1 (1991).
- ²C. Geibel, S. Thies, D. Kaczorowski, A. Mehner, A. Grauel, B. Seidel, U. Ahlheim, R. Helfrich, K. Petersen, C. D. Bredl, and F. Steglich, *Z. Phys. B* **83**, 305 (1991).
- ³R. Caspary, P. Hellmann, M. Keller, G. Sparn, C. Wassilew, R. Köhler, C. Geibel, C. Schank, F. Steglich, and N. E. Phillips, *Phys. Rev. Lett.* **71**, 2146 (1993).
- ⁴R. Feyerherm, A. Amato, F. N. Gygax, A. Schenck, C. Geibel, F. Steglich, N. Sato, and T. Komatsubara, *Phys. Rev. Lett.* **73**, 1849 (1994).
- ⁵P. Link, D. Jaccard, C. Geibel, C. Wassilew, and F. Steglich, *J. Phys. Condens. Matter* **7**, 373 (1995).
- ⁶K. Andres, J. E. Graebner, and H. R. Ott, *Phys. Rev. Lett.* **35**, 1779 (1975).
- ⁷A. de Visser, H. P. van der Meulen, L. T. Tai, and A. A. Menovsky, *Physica B* **199&200**, 100 (1994).
- ⁸A. Grauel, A. Böhm, H. Fischer, C. Geibel, R. Köhler, R. Modler, C. Schank, F. Steglich, G. Weber, T. Komatsubara, and N. Sato, *Phys. Rev. B* **46**, 5818 (1992).
- ⁹A. de Visser, H. Nakotte, L. T. Tai, A. A. Menovsky, S. A. M. Mentink, G. J. Nieuwenhuys, and J. A. Mydosh, *Physica B* **179**, 84 (1992).
- ¹⁰S. A. M. Mentink, T. E. Mason, S. Süllow, G. J. Nieuwenhuys, and J. A. Mydosh (unpublished).
- ¹¹A. Krimmel, P. Fischer, B. Roessli, H. Maletta, C. Geibel, C. Schank, A. Grauel, A. Loidl, and F. Steglich, *Z. Phys. B* **86**, 161 (1992).
- ¹²J. P. Desclaux and A. J. Freeman, in *Handbook on the Physics and Chemistry of the Actinides*, edited by A. J. Freeman and G. L. Lander (North-Holland, Amsterdam, 1984), Vol. 1, p. 46.
- ¹³C. Broholm, J. K. Kjems, W. J. L. Buyers, P. Matthews, T. T. M. Palstra, A. A. Menovsky, and J. A. Mydosh, *Phys. Rev. Lett.* **56**, 1467 (1987).
- ¹⁴L. M. Sandratskii, J. Kübler, P. Zahn, and I. Mertig, *Phys. Rev. B* **50**, 15 834 (1994).
- ¹⁵S. A. M. Mentink, G. J. Nieuwenhuys, A. A. Menovsky, J. A. Mydosh, H. Tou, and Y. Kitaoka, *Phys. Rev. B* **49**, 15 759 (1994).
- ¹⁶E. Bauer, R. Hauser, E. Gratz, G. Schaudy, M. Rotter, A. Lindbaum, D. Gignoux, and D. Schmitt, *Z. Phys. B* **92**, 411 (1993).